



Article citation info:

Pawlik P, Kania K, Przysucha B, Fault diagnosis of machines operating in variable conditions using artificial neural network not requiring training data from a faulty machine, *Eksploracja i Niezawodność – Maintenance and Reliability* 2023; 25(3) <http://doi.org/10.17531/ein/168109>

Fault diagnosis of machines operating in variable conditions using artificial neural network not requiring training data from a faulty machine

Indexed by:



Pawel Pawlik^{a,*}, Konrad Kania^b, Bartosz Przysucha^b

^a Department of Mechanics and Vibroacoustics, AGH University of Science and Technology, Poland

^b Department of Quantitative Methods in Management, Lublin University of Technology, Poland

Highlights

- It is possible to train a neural network with only data from an undamaged machine.
- The order spectrum of the novel parameter $rDPNS$ is proposed.
- The new method application for diagnosing unbalance and misalignment was analysed.
- Proposed architecture is resilient to overfitting without drop-outs and bagging.

Abstract

The fault diagnosis for maintenance of machines operating in variable conditions requires special dedicated methods. Variable load or temperature conditions affect the vibration signal values. The article presents a new approach to diagnosing rotating machines using an artificial neural network, the training of which does not require data from the damaged machine. This is a new approach not previously found in the literature. Until now, neural networks have been used for machine diagnosis in the form of classifiers, where data from individual faults were required. A new diagnostic parameter $rDPNS$ (Relative Differences Product of Network Statistics) as a function of the machine's shaft order was proposed as a kind of new order spectrum independent of the machine's operating conditions. The presented work analyses the use of the proposed method to diagnose misalignment and unbalance. The results of an experiment carried out in the laboratory demonstrated the effectiveness of the proposed method.

Keywords

fault diagnosis, vibroacoustic diagnostics, deep learning, neural networks, maintenance of technical systems.

This is an open access article under the CC BY license (<https://creativecommons.org/licenses/by/4.0/>)

1. Introduction

In the maintenance of rotating machinery, the vibration signal is the basis of condition monitoring systems. Dedicated signal analysis methods are applied depending on the technical object under investigation. An overview of methods for diagnosing planetary gears can be found in [1]. The vibration signal is often used in the diagnosis of rolling bearings, and several applications can be found in [2,3]. In a traditional condition monitoring approach following ISO 20816-1 [4], vibration measurement is required under fixed operating conditions of the machine. Unfortunately, this is often impossible to achieve in industrial conditions because a large group of machines operate

exclusively in variable conditions. In addition to any damage, the values of the parameters obtained using classic methods of vibration signal analysis are also affected by the operating conditions, i.e. changes in rotational speed, load, or oil temperature [5,6]. Many studies have been conducted in which the problem of eliminating the impact of changes in rotational speed and load condition on the vibration signal was addressed [7–9]. One way to do this is to use synchronous methods [10–12], which allow for the elimination of spectrum blur resulting from variable rotational speed [5]. However, variable operating conditions also affect the values of spectral amplitudes [13,14].

(*) Corresponding author.

E-mail addresses:

P. Pawlik (ORCID: 0000-0002-2654-6138) pawlik@agh.edu.pl, K. Kania (ORCID: 0000-0003-1545-0891) k.kania@pollub.pl, B. Przysucha (ORCID: 0000-0002-1117-8088) b.przysucha@pollub.pl,

Each operating condition factor affects the amplitude of diagnostic signals in a different way [15] and this requires the use of advanced signal analysis methods to separate the failure factors from the operating condition factors, given that the influence of these parameters can cause amplitude changes that can be interpreted by automatic monitoring systems as the presence of a fault. Vibration diagnostics can be carried out for fixed operating conditions, i.e. temperature, load, speed, to negate this effect. However, in industrial settings, in most cases ensuring fixed operating conditions is impossible to meet. The authors focused on the search for a method to diagnose machines operating at variable temperature and load.

In this work, a method based on the analysis of orders and artificial neural networks is proposed. A naturally occurring artificial intelligence model for diagnostic applications is that of classifier models. This is problematic, however, because when using neural networks as classifiers, learning data recorded for the machine to be diagnosed and for predicted faults are required [16–24]. There is work related to the reduction of damage data in learning vectors [25]. In industrial settings, acquiring measurement data for faults in a particular facility is difficult to achieve. Often, expensive expert inspections and preventive replacements are used to prevent faults from occurring, and this is especially true for machines that are unique in their design. As a result, the learning sets (necessary when using neural networks as classifiers) would contain a redundant representation of data from the undamaged machine relative to the data recorded during faults. There are review studies indicating that such unbalanced learning sets translate into poorer ability to classify underrepresented states [26–28]. In excess of this, even for objects of the same type, vibration signals can vary considerably due to imperfect workmanship. In addition, any new unforeseen damage may be misclassified. It is also possible to search for a damage model when creating diagnostic tools [29–32]; however, damage models in most cases require calibration with measurement data.

In the approach proposed by the authors, the artificial neural network model is not directly responsible for classifying the state of the machine. The regressive artificial neural network is trained only with data recorded during the fault-free operation, creating a reference model of the correct operation of the machine. This is a new approach not previously found in the

literature. Until now, neural networks have been used to diagnose machines in the form of classifiers, where data from individual faults were necessary. The authors emphasise that, as a result, the presented method allows diagnostics to be automated without the need for prior data collection from damaged machines.

The result of the applied method is the generation of values for a proposed diagnostic parameter $rDPNS$ (Relative Differences Product of Network Statistics) as a function of the shaft order. This allows for damage identification according to the theory of classical vibroacoustic diagnostics, based on spectral analysis. This solves another problem of using artificial intelligence for diagnostics as there is no need to predict particular types of damage in advance.

The next section presents a method for analysis of measurement signals in order to obtain input data for the artificial neural network. Section 3 contains a description of the applied architecture of the artificial neural network, the training method, the implementation of the neural network, and the method for obtaining the spectrum of diagnostic parameters. Section 4 describes the verification of the proposed method in the laboratory. Section 5 presents the results of the conducted diagnostic experiment.

2. Vibration signals analysis method

The proposed method for diagnosing rotary machines operating under variable loads is based on vibration acceleration, rotational speed, current intensity, and temperature measurements, with these signals being recorded synchronously. Then, the vibration signals are retested against the rotational speed signal of one of the shafts of the system. For this purpose, the order analysis method was used. In the first phase, the signal from the tachometer is subjected to the interpolation procedure using a cascaded integrator-comb CIC filter. Then, based on the filtered signal from the tachometer, a procedure of resampling the vibration signal is carried out in order to determine the vibration signal in relation to the angle of rotation (even angle signal). In the resampling method, time-samples are converted to angle samples. The time-samples are samples of the physical signal that are equally spaced in time. The angle samples are samples that are equally spaced in the rotation angle. The signal tested in this way can be subjected to

a rapid Fourier Transform (FFT), which results in a spectrum of orders. The order spectrum represents the amplitude as a function of orders and not as a function of frequency. The orders correspond to the multiple of the shaft frequency on which the rotational speed is measured [33]; in this case, the rotational speed is measured on the output shaft of the gearbox.

Analysis of orders also allows for observation of individual orders over time. By monitoring the amplitudes of characteristic orders, it is possible to obtain information about the technical condition of the tested object. However, a change in the amplitude value may also be caused by a change in the system load [34]. Thus, the order analysis makes it possible to compensate for changes in the frequency domain caused by variable loads. However, the question of the impact of the load on the signal amplitude remains. Therefore, this work attempted to develop a method that gives results independent of working conditions. The measurement of the load moment requires specialised apparatus, and in most cases is impossible to carry out in industrial conditions. However, assuming that the motor driving the system is powered by a constant frequency and amplitude voltage, which often occurs in industrial conditions, any change in speed will be caused by a changing load. Therefore, the rotational speed signal in this work will be used not only for resampling by the order analysis method but also for describing the impact of the load on vibration signals. Another indirect measurement method of the load moment is

the measurement of the current supplying the drive motor [35]. In the proposed method, the waveforms of both the current intensity and the rotational speed were taken as data describing the load change. Fig. 1 shows a signal processing algorithm for building vectors that teach an artificial neural network. At the input of the processing algorithm, signals of the vibration acceleration and the tachometer with a length of 30s are given. Then, the order analysis procedure is carried out using the method of testing the vibration signal with respect to the rotational speed of the shaft [33]. In the resampling method, time-samples are converted to angle samples. The time-samples are samples of the physical signal that are equally spaced in time; the angle samples are samples that are equally spaced in the rotation angle. The resampled signal undergoes a rapid Fourier Transform (FFT). The analysis of orders also allows us to obtain the waveforms of order amplitudes over time. In the next step n , the signals coming from n orders, as well as the temperature and current signals, are sorted in relation to the rotational speed of the machine shaft. The theoretical values of vibration signals should be repeatable for the same load conditions. The next step is to determine the moving mean for N subsequent elements. Averaging was used to reduce data dispersion. The data prepared were input vectors to the artificial neural network. The authors similarly prepared the data in their previous work [15].

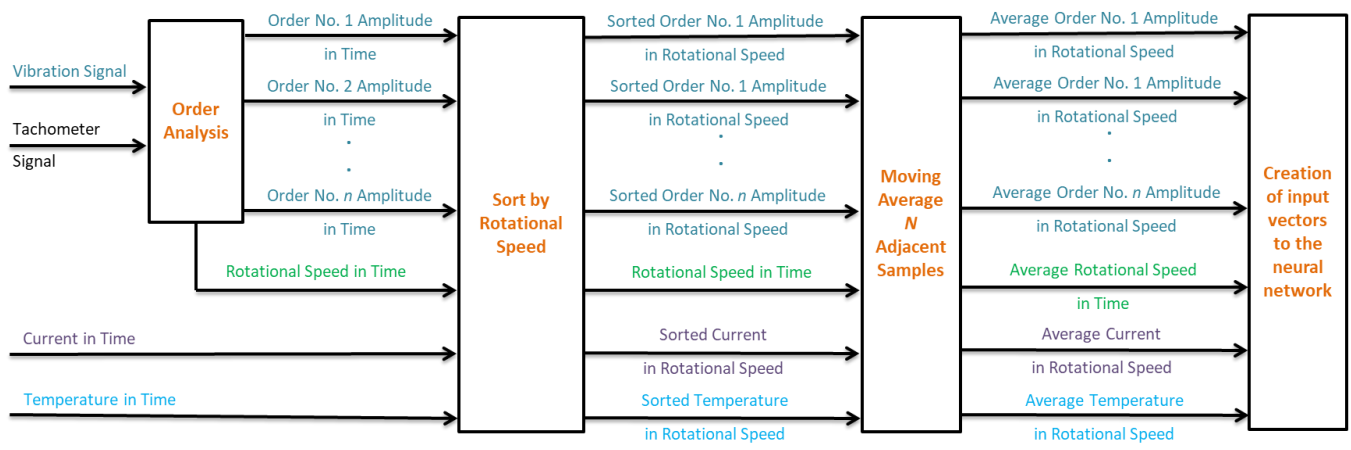


Fig. 1. Signal processing algorithm.

3. Neural network

3.1. Network architecture

In order to take into account the relationship between the values of the order spectrum and the operating conditions of the

machine, it was decided to use a deep neural network as a universal method, effectively approximating the complex relationships between the data [36–38]. In regression problem where the number of output variables is greater than the number of input variables, a common approach is to use an architecture

built from multiple neural networks, where the output variables are divided between several networks so that each of the subnetworks has more inputs than outputs. Such an approach has proved its effectiveness in solving inverse problems in tomography [39–41]. In the paper [15], results were published in which data on working conditions were treated as input data and attempts were made to recreate the values of the amplitudes of the order spectrum by modelling each of the orders separately. By complementing the models with techniques that make them resistant to overfitting, it was possible to obtain an architecture with satisfactory diagnostic and identification effectiveness, at the cost of needing to use a complex architecture consisting of 12,000 independently trained neural networks.

This paper proposes a new approach to recreating the relationship between working conditions and the spectrum of orders. Instead of predicting spectrum values based on the point of operation, a neural network was trained which treats the values of the order spectrum as input data and estimates the expected point of operation of the transmission based on them.

Such an approach allows us to build a single network with a large number of input variables in relation to the number of outputs, which allows us to obtain satisfactorily small estimation errors. In addition, thanks to the reversal of the estimation method, the need to use synthetic output data was removed, making the system resistant to the phenomenon of overfitting and eliminating the need to use bagging, which multiplied the number of neural networks needed to train the network. A diagram of the architecture of used multilayer fully-connected perceptron is presented in Fig. 2. The fundamental consideration in designing a neural network is its relatively small size to enable implementation in continuous monitoring systems. The number of input variables depends on the number of order amplitudes that we want to observe in the diagnosis process. In the case studied, the mesh order is No. 72, so 100 orders in two axes were analysed in order to observe the mesh modulation.

Model of the network and the training process was implemented in R programming language via Keras API.

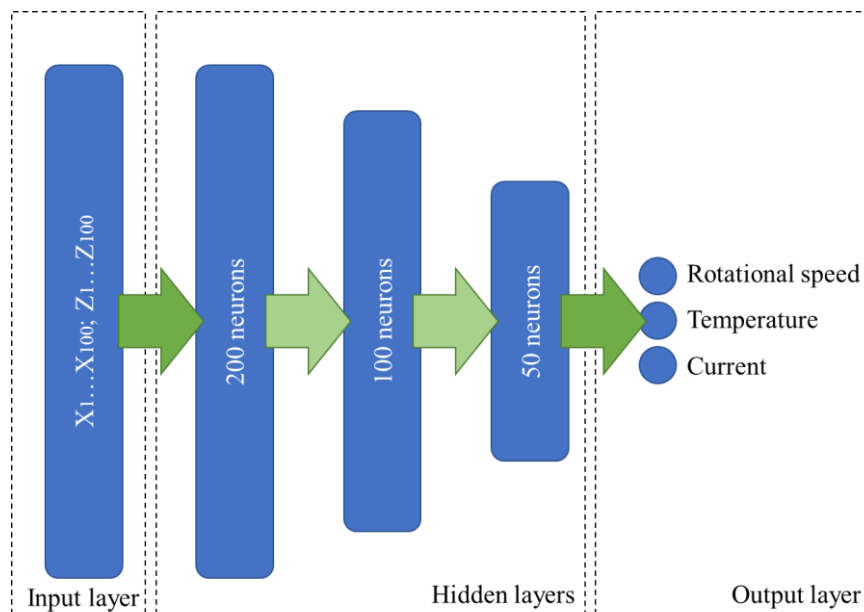


Fig. 2. The architecture of the applied neural network.

3.2. Network training

In industrial environments, data from damaged machines are difficult to access or scarce compared to data from undamaged machines because an industry strives to repair such machines as quickly as possible. Preventive replacement of parts is also practised (e.g. in the energy industry) to avoid the effects of a fault in the form of downtime, high costs, or disasters [42,43].

Another problem is the multitude of different types of damage that can occur in real machines, which will characterise a different nature of machine malfunctions. For these reasons, using classical machine learning methods is significantly more difficult, as they require collecting data sets containing predetermined types of damage. In addition, a small number of data cases with damage in training sets (in relation to fault-free

data) may negatively affect the model training process. In order to address these two fundamental problems, a revised approach to network training was applied, whereby the teaching set for a given neural network contained only data from an undamaged machine. In this way, the learned network will be a mathematical model of the undamaged machine. In general, the mechanism allowing for detecting faults consists in observing the differences between the measured machine parameters and the values predicted by the learned model. If the machine works faultlessly, the values from the model should be close to the measured values, while the increase in estimation errors suggests the appearance of damage.

The premise of the proposed method is that the training data should be determined from signals recorded for all possible ranges of operating conditions. Otherwise, signals for operating conditions not entered during network training could be interpreted as a fault during diagnosis. The fulfilment of this

condition is feasible because, usually in industrial conditions, the range of changes in the machine's operating conditions does not change during operation.

The data set from undamaged machine was divided into the training and test parts in an 80/20 percent ratio, and MSE (mean square error) was assumed as a function of the loss in the training process.

3.3. Using a trained network for diagnostics

The applied model allows for direct detection of a potential fault by observing the error scatter of the learned network. It is worth emphasising that while the technique based on comparing the error scatter allows for relatively simple detection of potential defects, it has limited identification capabilities. To detect and identify the defect, the authors propose to carry out an additional procedure allowing for the assessment of the discrepancy of network results for individual spectrum orders. The algorithm of this procedure is presented in Table 1.

Table 1. Procedure for determining the diagnostic parameter for individual orders.

Stage	Step	Action
Determination of parameters for the state without damage	1	Calculate network responses for the reference data (faultless)
	2	Swap values of amplitudes of the order i in the reference data with the analogous values from the training set
	3	Calculate responses for data after data swapping
	4	Calculate the vectors of differences between pre- and post-swapping responses
	5	Calculate the maximum norms of the obtained vectors of differences
	6	Determine the mean and variance of the obtained norms: $m_g(i), s_g^2(i)$
Determination of parameters for the state without damage	7	Calculate network responses for data examined for failure
	8	Swap values of amplitudes of the order i in the examined data with the analogous values from the reference set
	9	Calculate responses for data after data swapping
	10	Calculate the vectors of differences between pre- and post-swapping responses
	11	Calculate the maximum norms of the obtained vectors of differences
	12	Determine the mean and variance of the obtained norms: $m_f(i), s_f^2(i)$
Determination of the diagnostic parameter	13	Determine the diagnostic parameter $rDPNS(i)$ according to the formula (1)

3.4. Diagnostic parameter developed

As part of this work, the diagnostic parameter Relative Differences Product of Network Statistics ($rDPNS$) was developed (1), which is determined for each order separately:

$$rDPNS(i) = ReLU \left(\frac{s_f^2(i) - 2s_g^2(i)}{s_f^2(i) + 2s_g^2(i)} \right) \cdot ReLU \left(\frac{m_f(i) - m_g(i)}{m_f(i) + m_g(i)} \right) \quad (1)$$

where $s_f^2(i)$, $s_g^2(i)$, $m_g(i)$, $m_f(i)$ are the variances and means calculated according to the procedure in Table 1 and $ReLU$ is

Rectified Linear Unit:

$$ReLU(x) = \begin{cases} x & \text{if } x \geq 0 \\ 0 & \text{otherwise} \end{cases} \quad (2)$$

The parameter *rDPNS* proposed in this paper considers both the change in the mean value and the variance of the algorithm results from Table 1. Such a parameter was chosen because for signals originating from undamaged machine, an increase in the mean value and the variance in relation to these values for signals from the damaged machine was observed. In addition, due to differences in the values of variance for signals with and without faults, in order to ensure proper comparison, it was decided to compare the signal variance with faults with the doubled variance of signals without faults. In the case of means, no weights were used. The basic property of the measure proposed in this way is its limitedness – the value of the parameter will be in the range [0,1]. As the differences between examined and reference means and variances get greater, the value of the coefficient will be closer to one. For similar values, the coefficient value will approach zero. If any of the differences occurring in formula (1) is negative, the case is interpreted as the lack of defect. Because of that, the formula uses the *ReLU* function, which zeroes the *rDPNS* coefficient in such a situation. It is worth noting that the *ReLU* must be calculated separately for both factors in order to exclude a situation in which the product of two negative factors would result in a positive coefficient value.

The use of a measure whose values fall within the range [0,1] allows for the use of the effect size scale. It was decided

to use the Cohen [44] scale mainly used for qualitative variables, which also works perfectly for other coefficients [15].

The Cohen scale is as follows:

Table 2. Cohen Scale.

Range of parameter	The Power of the Effect
0–0.1	No effect
0.1–0.3	Little effect
0.3–0.5	Medium effect
0.5–1.0	Large effect

Determining the *rDPNS* parameter for each order individually allows for the identification of potential faults in accordance with the classic spectral analysis of the vibration signal. For example, changes in the value for order 1 will be caused by unbalance of the machine shaft. Changes in the value for order 2 will be caused by shifts in placement between rigidly connected machines [45]. However, for couplings, it will be an order corresponding to the number of coupling gears.

4. Experimental validation

In order to validate the proposed method of diagnosis, an experiment was carried out on a laboratory stand for diagnosing planetary gears.

4.1. Rig design

The laboratory stand (Fig. 3) consists of an electric motor driving (1) a TRAMEC EP 90/1 planetary gearbox (2), which was then connected using a jaw coupling (3) with a second motor acting as a load (4). Frequency converters (5) controlled both the driving and braking motors. The converters allow for any function of rotational speed and load.

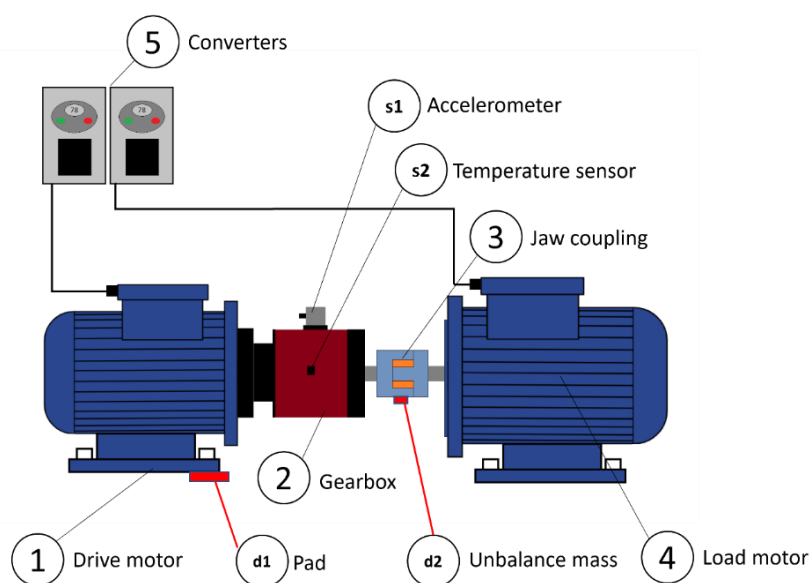


Fig. 3. Schematic drive train.

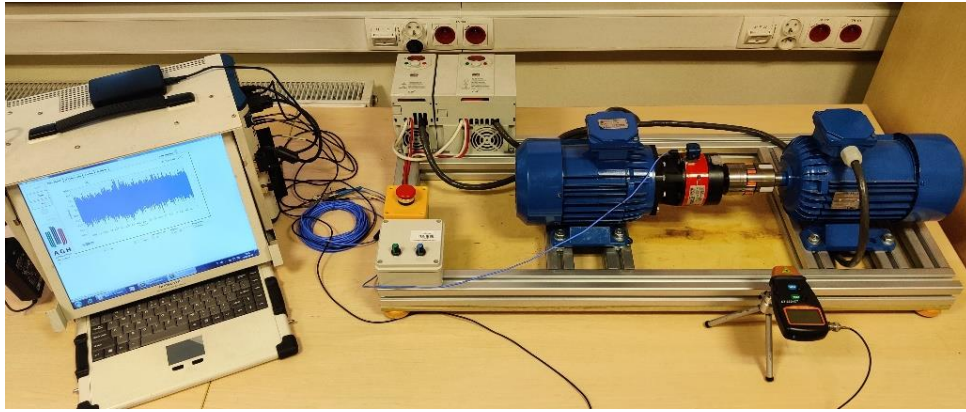


Fig. 4. Real drive train.

A three-axis vibration acceleration sensor PCB 356B08 and a temperature sensor LM35 are mounted on the transmission housing. The rotational speed was measured using a laser tachometer, while the current intensity was measured using an ACS714 sensor. The recording of the measurement signals and the signal processing algorithm were carried out in a dedicated application built in the LabVIEW environment. Fig. 4 shows a photo of the laboratory stand.

4.2. Experimental methodology

In order to verify the effectiveness of the trained network in diagnosis, faults were introduced in the laboratory bench. Measurements were carried out for four states of the drive system, without damage, for misalignment between the transmission and the braking motor, unbalance, and simultaneous unbalance and misalignment.

Table 3. Designation and measurement time for individual states of the drive system.

Designation	Condition of the machine	Measurement time
S0	no damage	30 min
S1	misalignment	30 min
S2	unbalance	30 min
S3	misalignment and unbalance	30 min

The state of misalignment (S1) consisted in placing washers 0.5mm thick under the front feet of the drive motor. The place where the washers were mounted is marked on Fig. 3 (d1). Unbalance (S2) was introduced by placing an additional mass (3g) on the output shaft coupling (Fig. 3) (d2). The state of S3 consisted in the simultaneous introduction of misalignment and unbalance. For each state, signals with a length of 30 min were recorded. In order to examine the influence of temperature on vibration signals, measurements were also carried out while heating the system for a temperature in the range of 35–40 °C.

After each state, the machine was switched off until it cooled down to ambient temperature.

The system was subjected to a load corresponding to the load occurring on the main gear of the bucket wheel excavator but scaled to the capabilities of the laboratory stand. The reference signal was obtained from the monitoring system of the main gearbox of a KWK 1500s excavator. The gearbox included in the laboratory stand was loaded in the range of 1.3 Nm to 4.0 Nm, which resulted in changes in the rotational speed in the range of 730–758 RPM. The course of rotational speed changes is shown in Fig. 5. With a constant set voltage value on the drive motor, the load causes a change in rotational speed and vibration amplitude.

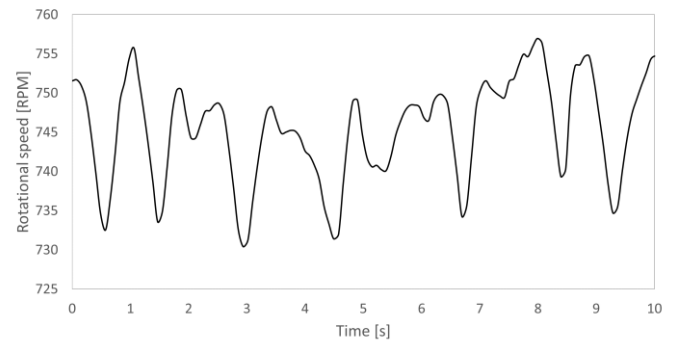


Fig. 5. Output shaft rotational speed waveform.

5. Results

The results were analysed using order analysis alone, and the dependence of the spectrum of orders on load and temperature is presented. Next, the results of the neural network for the data from the experiment are presented, and the values of the proposed *rDPNS* parameter in the order function are presented.

5.1. Order analysis

In the case of machines operating under variable load or

rotational speed, synchronous methods are used. One popular tool is the order spectrum, however order spectrum analysis may not be a sufficient tool to assess technical conditions in high load variability. Fig. 6 shows the spectrum of vibration acceleration orders for the system without damage (black) and for the system with misalignment.

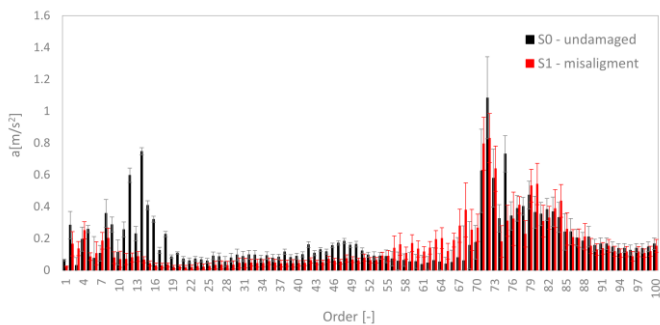


Fig. 6. The spectrum of vibration acceleration orders for the system without damage (black) and for the system with misalignment (red).

Misalignment of the system with the jaw coupling results in

changes for the order corresponding to the number of claws (order 4), its multiples, and the frequency of meshing (order 72). Observing the spectrum of orders, the differences for orders 4 and 8 are not significant, while the amplitude of the order of meshing decreases with the damage. In this case, the misalignment might not be detected using the averaged order spectrum. The error bars represent the standard deviation of the amplitude caused by the system's variable load.

The short-time order spectra as a function of rotational speed caused by the load change are shown in Fig. 7. The left side shows the spectrum for the system without damage, while the right side shows the spectrum for the system with the introduced misalignment. Significant differences in the values of the spectrum amplitudes caused by the load can be observed both for the efficient system and the one with damage introduced. However, there is a significant change in the nature of the dependence of the amplitudes of the orders on the rotational speed (caused by the change in load), especially for the meshing band of the diagnosed machine (64–80 orders).

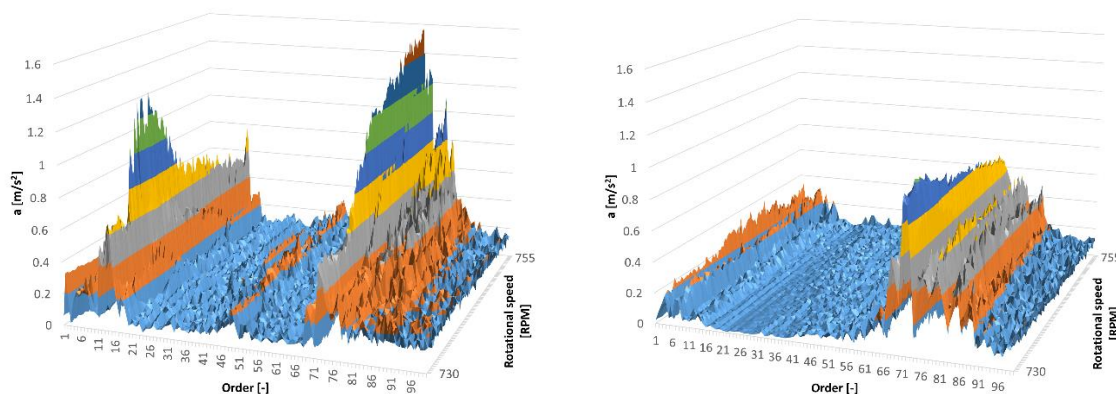


Fig. 7. Spectrum of vibration acceleration orders as a function of rotational speed, for the system without damage (left) and for the system with misalignment (right), temperature 36.2 °C.

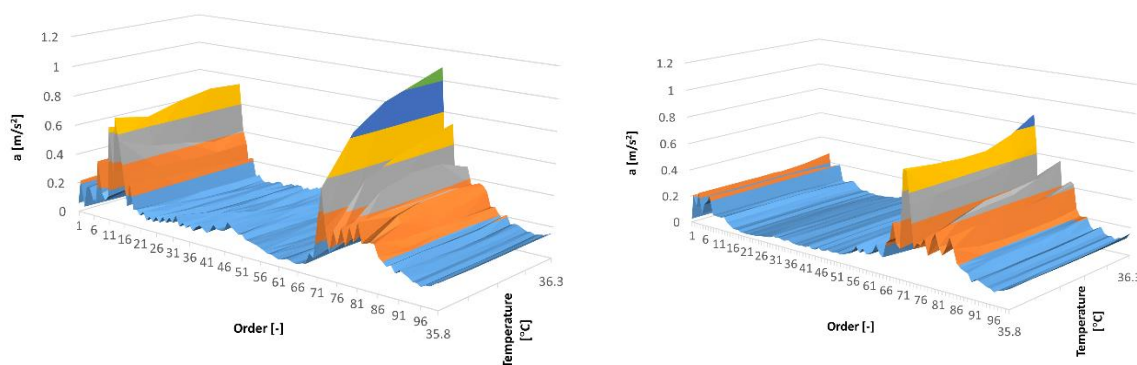


Fig. 8. The spectrum of vibration acceleration orders as a function of temperature, for the system without damage (left) and for the system with misalignment (right).

The oil temperature also influences the amplitude of vibrations generated by the gearbox. Fig. 8 shows the spectra of the orders as a function of the temperature measured on the gear body. A significant impact on the vibration acceleration amplitude values is visible, especially in the meshing band (64–80 orders).

5.2. Scatter plots of errors

The error scatter of individual network output values was analysed. Fig. 9 shows a graph of the error scatter of network

output values for the test data compared to the error scatter for the training data, while Fig. 10 compares analogous graphs for data with the considered faults introduced.

Fig. 9 shows that introducing new faultless data into the network results in the fact that the observable scatter of estimation errors remain at a level similar to that observed for the training data. This means that the network has correctly learnt to recognise faultless operation states, and the model is not overfitted.

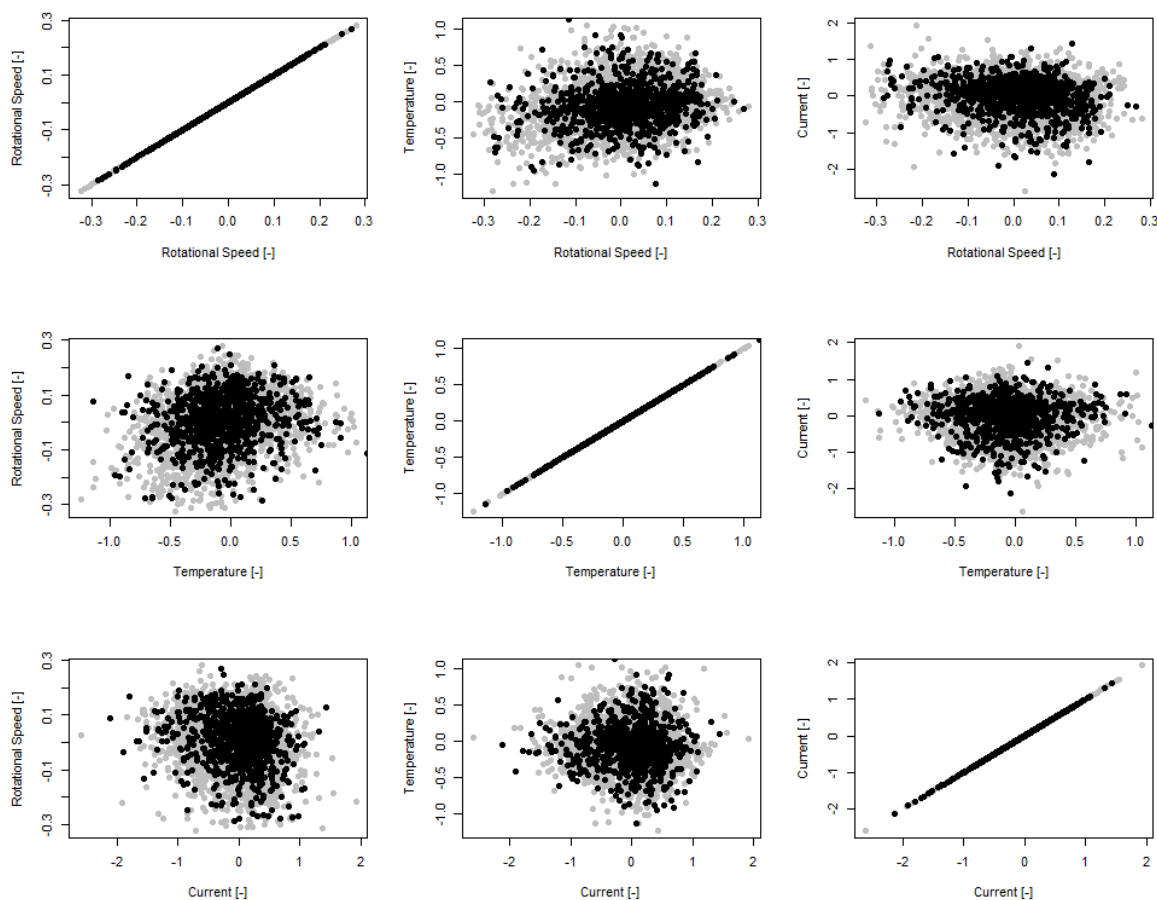


Fig. 9. Scatter of network output estimation error for faultless data. The output was subject to standardisation. Data from the test set (black), data from the training set (grey).

On the other hand, as shown in Fig. 10, when we transfer data from the damaged system to the network, the neural network estimation error scatter increases noticeably. Since the network was taught the nature of fault-free system, the increase in the error scatter must mean that the nature of the machine deviates from the normal one, suggesting the occurrence of a fault. Overall, the smallest increases in scatter were observed for unbalance, which, given the nature of this defect, was the expected result, because unbalance causes amplitude changes

only for order 1. Nevertheless, this increase, especially in the case of temperature, is so visible that it allows us to effectively distinguish it from the point cloud corresponding to faultless data. Misalignment occurred to be easier to detect; the neural network estimation error cloud for misalignment or misalignment with unbalance is significantly larger than that for faultless data. In addition, the difference in the error of determining the temperature, when we add the unbalance to the misalignment, is so noticeable that it allows us to distinguish the

two states from one another. It is also interesting that while the unbalance alone increases the temperature estimation error, in the case of co-existence with the misalignment, the unbalance

seems to cause a decrease in the temperature estimation error in relation to the error when the misalignment occurs on its own.

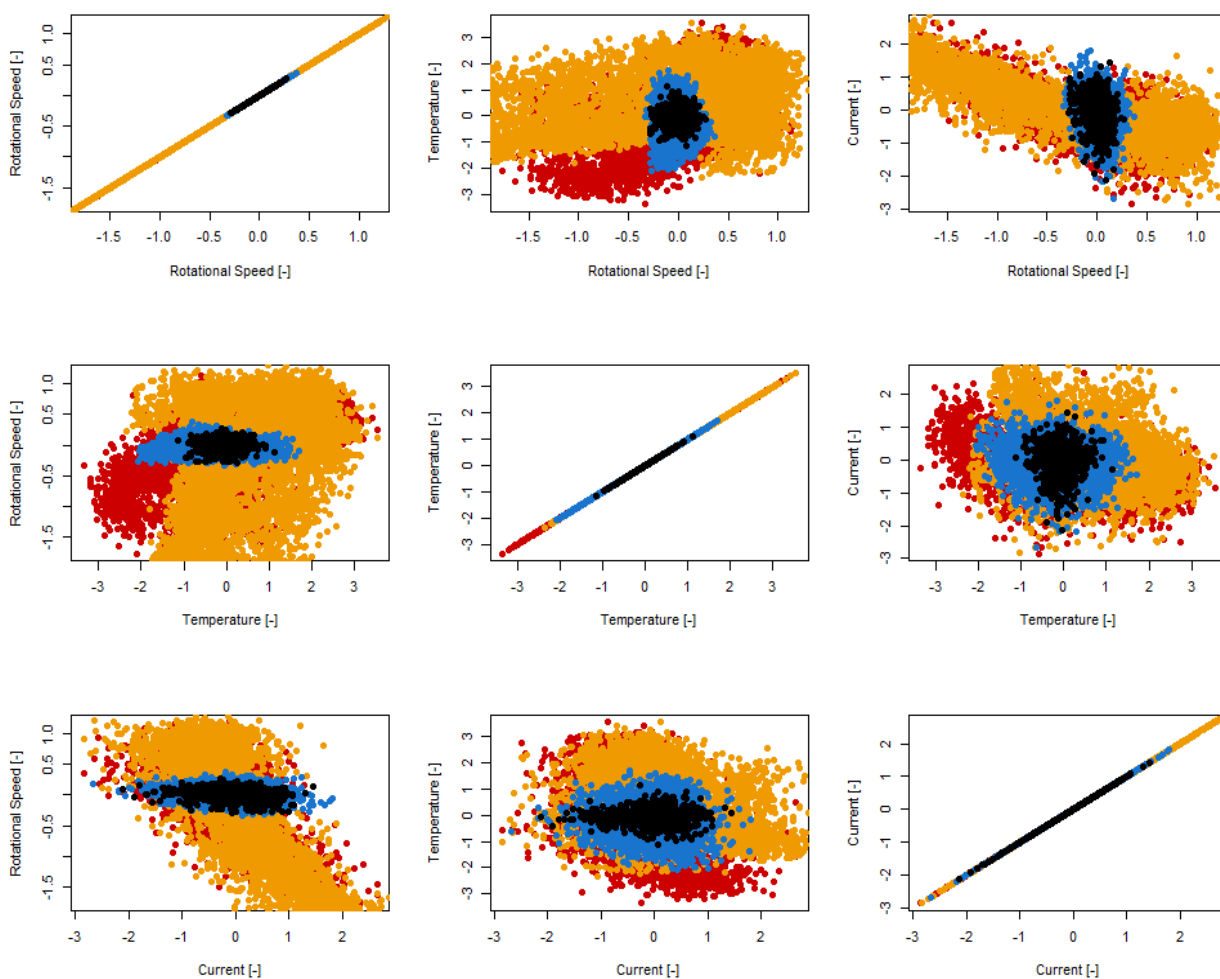


Fig. 10. Scatter of network output estimation error for fault data. The output values were subject to standardisation. Fault-free – test data (black), unbalance (blue), misalignment (red), misalignment and unbalance (orange).

5.3. Neural network

This section presents the graphs of the *rDPNS* parameter as a function of the order, determined following the algorithm presented in Table 1. Fig.11 shows the spectrum for the misalignment state (S1). According to the theory of diagnostics, the misalignment causes an increase in order amplitude corresponding to the number of claws (4). The *rDPNS* parameter value for order 4 is in the range of 0.3–0.5, which indicates a medium effect according to the Cohen scale. Significant values (> 0.5) are adopted by *rDPNS* in the range of meshing (68–76 orders) because misalignment also affects the way the gears mesh [46].

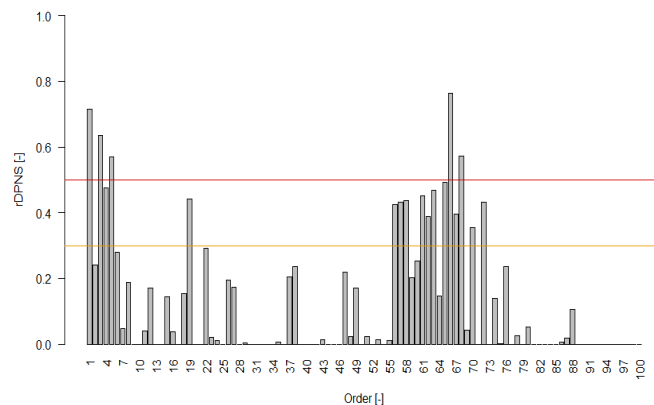


Fig. 11. Spectrum of orders of parameter *rDPNS* for state S1 (misalignment).

The values of $rDPNS$ for the unbalance state (S2) are shown in Fig. 12. According to the Cohen scale, a large effect can be observed only for order 1. This is consistent with the theory of diagnostics regarding the unbalance of rotating elements. Order 1 corresponds to the rotational frequency of the shaft on which the unbalance occurred. Observing the spectrum, it can be clearly stated that there is an unbalance.

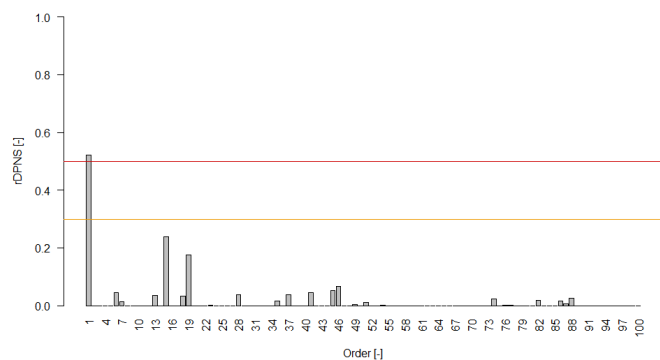


Fig. 12. Spectrum of orders of parameter $rDPNS$ for state S2 (unbalance).

For the state S3 corresponding to misalignment and unbalance, the values indicating a large effect occur both for order 1 and for orders from the mesh band (Fig. 13). The order spectrum of the parameter $rDPNS$ looks very similar as in the case of S1; however, there are symptoms related to misalignment (order 4 and orders 68–76) and unbalance (order 1).

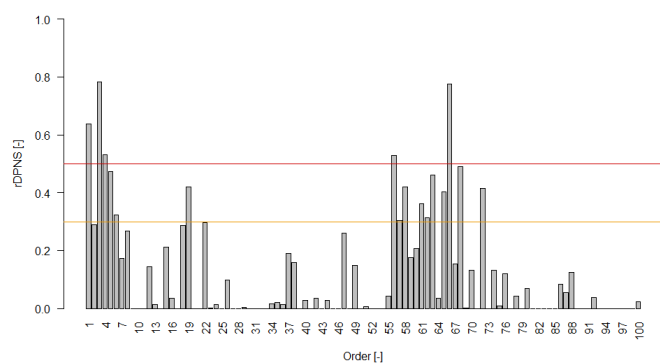


Fig. 13. Spectrum of orders of parameter $rDPNS$ for state S3 (misalignment and unbalance).

6. Conclusions

This study addressed the diagnosis of machines operating in variable conditions using artificial neural networks trained only with signals from an undamaged machine. The influence of the load and oil temperature on the amplitude values of the spectrum of orders was analysed.

A method of diagnosis based on the analysis of orders and an artificial neural network that does not require learning data from the faulty machine has been proposed. This is a new approach not previously found in the literature. So far, neural networks have been used in diagnosis in the form of classifiers, where training data attributed to the faults in question were required. For this reason, the presented technique can be considered as an unsupervised method from the point of view of machine learning theory, which significantly facilitates its application in industrial conditions. The trained, deep neural network mapped the relationships between the values of amplitudes in the spectrum of orders (constituting the input variables of the network) and the rotational speed, oil temperature, and current, which constituted the output variables. This paper proposes a new approach to illustrating the relationship between working conditions and the spectrum of orders. It has been shown that in the event of damage, there is an increase in errors in the estimation of the network trained to predict the operating conditions in the faultless operation of the drive.

In order to identify emerging faults, a procedure for analysing the neural network response was proposed, allowing us to generate the $rDPNS$ diagnostic parameter in the form of a normalised spectrum. The normalised spectrum allows for use in automatic monitoring systems. The $rDPNS$ parameter proposed in the paper allows for the determination of the size of the potential damage effect on the characteristics of each order. As a result, it allows us to obtain a spectrum of orders of the $rDPNS$ parameter, which can be interpreted in accordance with the theory of vibroacoustic diagnostics. This spectrum is resistant to interference introduced by variable operating conditions (e.g. load, oil temperature).

In order to verify the correctness of the proposed method, an experiment was carried out on a laboratory stand, and the possibility of detecting misalignment, unbalance and misalignment and unbalance at the same time was analysed. In the case of misalignment, a large effect of the $rDPNS$ parameter failure was observed for orders corresponding to this damage. Similarly, in the case of unbalance, a large effect was observed for the $rDPNS$ corresponding to order 1. However, in the case of simultaneous misalignment and unbalance, a spectrum of orders of the $rDPNS$ parameter was obtained similar to the state

of misalignment alone. However, there is also a large effect on the parameter corresponding to order 1.

The conducted experiment proves that the presented method allows for the potential identification of a wide range of various types of faults without the need to take into account – at the system design stage – which faults are to be captured. In addition, by presenting the results in the form of a standardised

spectrum, the result of the analysis is intuitive for diagnostics specialists or interpretable by automatic systems, which is another aspect facilitating the implementation of such a technique in industrial conditions.

Further experiments will address the potential of using other network models to reduce the computational complexity of the entire procedure.

Acknowledgements

This work was supported by the Polish Ministry of Science and Higher Education [grant number 16.16.130.942].

Author Contributions

Conceptualization, P.P. and K.K.; methodology, P.P., K.K. and B.P.; software, P.P. and K.K.; validation, P.P., K.K. and B.P.; formal analysis, P.P., K.K. and B.P.; investigation, P.P.; resources, P.P. and K.K.; data curation, P.P. and K.K.; writing—original draft preparation, P.P., K.K. and B.P.; writing—review and editing, P.P., K.K. and B.P.; visualization, P.P. and K.K.; supervision, P.P.; project administration, P.P.; funding acquisition, P.P. and B.P. All authors have read and agreed to the published version of the manuscript.

References

1. Lei Y, Lin J, Zuo M J, He Z. Condition monitoring and fault diagnosis of planetary gearboxes: A review. *Measurement* 2014;48:292–305. <https://doi.org/10.1016/j.measurement.2013.11.012>.
2. Tandon N, Choudhury A. A review of vibration and acoustic measurement methods for the detection of defects in rolling element bearings. *Tribol Int* 2000;32:469–80. [https://doi.org/10.1016/S0301-679X\(99\)00077-8](https://doi.org/10.1016/S0301-679X(99)00077-8).
3. Randall R B, Antoni J. Rolling element bearing diagnostics-A tutorial. *Mech Syst Signal Process* 2011;25:485–520. <https://doi.org/10.1016/j.ymsp.2010.07.017>.
4. ISO/TC 108/SC 2. ISO - ISO 20816-1:2016 - Mechanical vibration — Measurement and evaluation of machine vibration — Part 1: General guidelines. 2016.
5. Randall R B. Vibration-based diagnostics of gearboxes under variable speed and load conditions. *Meccanica* 2016;51:3227–39. <https://doi.org/10.1007/s11012-016-0583-z>.
6. Antoniadou I, Manson G, Staszewski W J, Barszcz T, Worden K. A time–frequency analysis approach for condition monitoring of a wind turbine gearbox under varying load conditions. *Mech Syst Signal Process* 2015;64–65:188–216. <https://doi.org/10.1016/j.ymsp.2015.03.003>.
7. Chen Z, Chen J, Xie Z, Xu E, Feng Y, Liu S. Multi-expert Attention Network with Unsupervised Aggregation for long-tailed fault diagnosis under speed variation 2022;252:109393. <https://doi.org/10.1016/j.knosys.2022.109393>.
8. Wang X, Zheng J, Ni Q, Pan H, Zhang J. Traversal index enhanced-gram (TIEgram): A novel optimal demodulation frequency band selection method for rolling bearing fault diagnosis under non-stationary operating conditions. *Mech Syst Signal Process* 2022;172:109017. <https://doi.org/10.1016/J.YMSSP.2022.109017>.
9. Guan Y, Liang M, Neculescu D S. Velocity synchronous bilinear distribution for planetary gearbox fault diagnosis under non-stationary conditions. *J Sound Vib* 2019;443:212–29. <https://doi.org/10.1016/J.JSV.2018.11.039>.
10. Gade S, Herlufsen H, Konstantin-Hansen H, Wismer N J. Order Tracking Analysis. vol. 2. Nærum: Brüel & Kjær; 1995.
11. Borghesani P, Pennacchi P, Randall R B, Ricci R. Order tracking for discrete-random separation in variable speed conditions. *Mech Syst Signal Process* 2012;30:1–22. <https://doi.org/10.1016/j.ymsp.2012.01.015>.
12. Fyfe K R, Munck E D S. Analysis of computed order tracking. *Mech Syst Signal Process* 1997;11:187–205. <https://doi.org/10.1006/mssp.1996.0056>.
13. Bartelmus W, Zimroz R. A new feature for monitoring the condition of gearboxes in non-stationary operating conditions. *Mech Syst Signal Process* 2009;23:1528–34. <https://doi.org/10.1016/j.ymsp.2009.01.014>.

14. Cheng W, Gao R X, Wang J, Wang T, Wen W, Li J. Envelope deformation in computed order tracking and error in order analysis. *Mech Syst Signal Process* 2014;48:92–102. <https://doi.org/10.1016/j.ymsp.2014.03.004>.
15. Pawlik P, Kania K, Przystała B. The Use of Deep Learning Methods in Diagnosing Rotating Machines Operating in Variable Conditions. *Energies (Basel)* 2021;14:4231. <https://doi.org/10.3390/EN14144231>.
16. Kumar A, Gandhi C P, Zhou Y, Kumar R, Xiang J. Latest developments in gear defect diagnosis and prognosis: A review. *Measurement* 2020;158:107735. <https://doi.org/10.1016/j.measurement.2020.107735>.
17. Zuber N, Bajrić R. Gearbox faults feature selection and severity classification using machine learning. *Eksploatacja i Niezawodność – Maintenance and Reliability* 2020;22:748–56. <https://doi.org/10.17531/ein.2020.4.19>.
18. Ilić D, Milošević D, Jovanović Z, Cvjetković M, Vulić M. MLP ANN Condition Assessment Model of the Turbogenerator Shaft A6 HPP Đerdap 2. *Technical Gazette* 2021;28:291–6. <https://doi.org/10.17559/TV-20190510052210>.
19. Vinokur A I, Kulikov G B, Suslov M V, Petrov V P, Bykov A V, Litunov S N, et al. Diagnostics of rolling bearings using artificial neural networks. *J Phys Conf Ser* 1901:12027. <https://doi.org/10.1088/1742-6596/1901/1/012027>.
20. Haj Mohamad T, Nataraj C, Haj Mohamad T, Nataraj C. Gear Fault Diagnostics Using Extended Phase Space Topology. *Annual Conference Of The Prognostics And Health Management Society*, 2017, p. 1–9. <https://doi.org/10.1115/1.4040041>.
21. Soualhi M, Nguyen K T P, Soualhi A, Medjaher K, Hemsas K E. Health monitoring of bearing and gear faults by using a new health indicator extracted from current signals. *Measurement (Lond)* 2019;141:37–51. <https://doi.org/10.1016/j.measurement.2019.03.065>.
22. Afia A, Rahmoune C, Benazzouz D, Merainani B, Fedala S. New intelligent gear fault diagnosis method based on Autogram and radial basis function neural network. *Advances in Mechanical Engineering* 2020;12:1–15. <https://doi.org/10.1177/1687814020916593>.
23. Dabrowski D. Condition monitoring of planetary gearbox by hardware implementation of artificial neural networks. *Measurement (Lond)* 2016;91:295–308. <https://doi.org/10.1016/j.measurement.2016.05.056>.
24. Kozłowski E, Borucka A, Świdorski A, Skoczyński P. Classification Trees in the Assessment of the Road–Railway Accidents Mortality. *Energies* 2021, Vol 14, Page 3462 2021;14:3462. <https://doi.org/10.3390/EN14123462>.
25. Su H, Yang X, Xiang L, Hu A, Xu Y. A novel method based on deep transfer unsupervised learning network for bearing fault diagnosis under variable working condition of unequal quantity. *Knowl Based Syst* 2022;242:108381. <https://doi.org/10.1016/J.KNOSYS.2022.108381>.
26. Wang L, Han M, Li X, Zhang N, Cheng H. Review of Classification Methods on Unbalanced Data Sets. *IEEE Access* 2021;9:64606–28. <https://doi.org/10.1109/ACCESS.2021.3074243>.
27. Konno T, Iwazume M. Cavity Filling: Pseudo-Feature Generation for Multi-Class Imbalanced Data Problems in Deep Learning 2018. <https://doi.org/10.48550/arxiv.1807.06538>.
28. Lin L, Guo S. Text Classification Feature Extraction Method Based on Deep Learning for Unbalanced Data Sets. *Lecture Notes of the Institute for Computer Sciences, Social-Informatics and Telecommunications Engineering, LNICST* 2021;347:320–31. https://doi.org/10.1007/978-3-030-67871-5_29/COVER.
29. Gecgel O, Ekwaro-Osire S, Dias J P, Serwadda A, Alemayehu F M, Nispel A. Gearbox Fault Diagnostics Using Deep Learning with Simulated Data. *IEEE International Conference on Prognostics and Health Management (ICPHM)* 978-1-5386-8357-6/19/\$31.00 ©2019 IEEE, 2019. <https://doi.org/10.1109/ICPHM.2019.8819423>.
30. Rymarczyk T, Przystała B, Pawlik P. Analysis of multi-source data for monitoring and control of intelligent technological systems. *Przegląd Elektrotechniczny* 2020;1:97–100. <https://doi.org/10.15199/48.2020.09.20>.
31. Peruń G, Łazarz B. Modelling of Power Transmission Systems for Design Optimization and Diagnostics of Gear in Operational Conditions. *Solid State Phenomena* 2014;210:108–14. <https://doi.org/10.4028/www.scientific.net/SSP.210.108>.
32. Kozłowski E, Borucka A, Liu Y, Mazurkiewicz D. Conveyor Belts Joints Remaining Life Time Forecasting with the Use of Monitoring Data and Mathematical Modelling. In: Machado J, Soares F, Trojanowska J, Yildirim S, editors. *Innovations in Mechatronics Engineering*, Springer Science and Business Media Deutschland GmbH; 2022, p. 44–54. https://doi.org/10.1007/978-3-030-79168-1_5/COVER.
33. National Instruments Corporation. *LabVIEW, Order Analysis Toolkit User Manual*. Austin, Texas: 2005.
34. Cempel C. Application of TRIZ approach to machine vibration condition monitoring problems. *Mech Syst Signal Process* 2013;41:328–34. <https://doi.org/10.1016/j.ymsp.2013.07.011>.

35. Nakamura T, Okuno M, Yoshikawa M, Itoh Y. Quantitative characterization of nonlinear impedance and load characteristic of 50-kW-class fully superconducting induction/synchronous motor. *Physica C: Superconductivity and Its Applications* 2020;578:1353662. <https://doi.org/10.1016/J.PHYSC.2020.1353662>.
36. McCann M T, Jin K H, Unser M. Convolutional neural networks for inverse problems in imaging: A review. *IEEE Signal Process Mag* 2017;34:85–95. <https://doi.org/10.1109/MSP.2017.2739299>.
37. Lin S B. Limitations of shallow nets approximation. *Neural Networks* 2017;94:96–102. <https://doi.org/10.1016/J.NEUNET.2017.06.016>.
38. Guo Z C, Shi L, Lin S B. Realizing Data Features by Deep Nets. *IEEE Trans Neural Netw Learn Syst* 2020;31:4036–48. <https://doi.org/10.1109/TNNLS.2019.2951788>.
39. Kłosowski G, Rymarczyk T, Kania K, Świć A, Cieplak T. Maintenance of industrial reactors supported by deep learning driven ultrasound tomography. *Eksploatacja i Niezawodność – Maintenance and Reliability* 2020;22:138–47. <https://doi.org/10.17531/ein.2020.1.16>.
40. Rymarczyk T, Kłosowski G. Innovative methods of neural reconstruction for tomographic images in maintenance of tank industrial reactors. *Eksploatacja i Niezawodność* 2019;21:261–7. <https://doi.org/10.17531/EIN.2019.2.10>.
41. Rymarczyk T, Kłosowski G. Applying Machine Learning Algorithms to Solve Inverse Problems in Electrical Tomography. *MATEC Web of Conferences* 2018;210:02016. <https://doi.org/10.1051/mateconf/201821002016>.
42. Utne I B. Maintenance strategies for deep-sea offshore wind turbines. *Journal of Quality in Maintenance Engineerin* 2010;16:367–81. <https://doi.org/10.1108/13552511011084526>.
43. Schuh P, Schneider D, Funke L, Tracht K. Cost-optimal spare parts inventory planning for wind energy systems. *Logistics Research* 2015;8:1–8. <https://doi.org/10.1007/S12159-015-0122-7/FIGURES/4>.
44. Cohen J. *Statistical Power Analysis for the Behavioral Sciences* Second Edition. New York: Lawrence Erlbaum Associates; 1988.
45. Lees A W. Misalignment in rigidly coupled rotors. *J Sound Vib* 2007;305:261–71. <https://doi.org/10.1016/j.jsv.2007.04.008>.
46. Kumar P, Hirani H. Misalignment effect on gearbox failure: An experimental study. *Measurement* 2021;169:108492. <https://doi.org/10.1016/J.MEASUREMENT.2020.108492>.